3 Biotech (2020) 10:258
https://doi.org/10.1007/s13205-020-02223-3

ORIGINAL ARTICLE

Optimization of the L-tyrosine metabolic pathway in *Saccharomyces cerevisiae* by analyzing *p*-coumaric acid production

Yuanzi Li[1] · Jiwei Mao[2] · Xiaofei Song[1] · Yuzhen Wu[1] · Miao Cai[1] · Hesuiyuan Wang[1] · Quanli Liu[2] · Xiuming Zhang[1] · Yanling Bai[1] · Haijin Xu[1] · Mingqiang Qiao[1]

Received: 31 July 2019 / Accepted: 24 April 2020 / Published online: 18 May 2020

Abstract

In this study, we applied a series of genetic modifications to wild-type *S. cerevisiae* strain BY4741 to address the bottlenecks in the L-tyrosine pathway. A tyrosine ammonia-lyase (TAL) gene from *Rhodobacter capsulatus*, which can catalyze conversion of L-tyrosine into *p*-coumaric acid, was overexpressed to facilitate the analysis of L-tyrosine and test the strain's capability to synthesize heterologous derivatives. First, we enhanced the supply of precursors by overexpressing transaldolase gene *TAL1*, enolase II gene *ENO2*, and pentafunctional enzyme gene *ARO1* resulting in a 1.55-fold increase in *p*-coumaric acid production. Second, feedback inhibition of 3-deoxy-D-arabino-heptulosonate-7-phosphate synthase and chorismate mutase was relieved by overexpressing the mutated feedback-resistant $ARO4^{K229L}$ and $ARO7^{G141S}$, and a 3.61-fold improvement of *p*-coumaric acid production was obtained. Finally, formation of byproducts was decreased by deleting pyruvate decarboxylase gene *PDC5* and phenylpyruvate decarboxylase gene *ARO10*, and *p*-coumaric acid production was increased 2.52-fold. The best producer—when *TAL1*, *ENO2*, *ARO1*, $ARO4^{K229L}$, $ARO7^{G141S}$, and *TAL* were overexpressed, and *PDC5* and *ARO10* were deleted—increased *p*-coumaric acid production by 14.08-fold (from 1.4 to 19.71 mg L^{-1}). Our study provided a valuable insight into the optimization of L-tyrosine metabolic pathway.

Keywords L-Tyrosine · Metabolic engineering · *p*-Coumaric acid · *Saccharomyces cerevisiae*

Introduction

The plant secondary metabolites flavonoids, stilbenoids and alkaloids have attracted increasing attention due to their pharmaceutical and nutritional applications (Akinwumi et al. 2018; Chougule et al. 2011; Yao et al. 2004). They are mainly obtained by extraction from plants and the extraction is energy intensive, inefficient and not environmentally friendly (Donnez et al. 2009; Sato et al. 2007; Silva et al. 2017). Heterologous biosynthesis in engineered microbes may be a good choice to achieve low consumption of energy and high yield of these secondary metabolites (Xu et al. 2013). To maximize product yield, two general strategies are often used: optimization of heterologous pathways; and improvement of plant secondary metabolite precursors in host cells. Because L-tyrosine is a common precursor for many plant secondary metabolites, it is vital to optimize its metabolic pathway.

Saccharomyces cerevisiae is often chosen as the microbial host for the production of heterologous compounds, due to its safe use status in food industry and in pharmaceutical biotechnology, its high amenability to genetic manipulation, and its eukaryotic nature, which may be helpful for the functional expression of plant-derived enzymes, such as cytochrome P450 enzymes (Borodina and Nielsen 2014; Jiang and Morgan 2004; Krivoruchko and Nielsen 2015). CEN.PK and BY4741 are the two most

Electronic supplementary material The online version of this article (https://doi.org/10.1007/s13205-020-02223-3) contains supplementary material, which is available to authorized users.

✉ Haijin Xu
xuhaijin@aliyun.com

✉ Mingqiang Qiao
qiaomq@nankai.edu.cn

[1] The Key Laboratory of Molecular Microbiology and Technology, Ministry of Education, College of Life Sciences, Nankai University, No. 94 Weijin Road, Nankai District, Tianjin 300071, People's Republic of China

[2] Department of Biology and Biological Engineering, Chalmers University of Technology, 41296 Gothenburg, Sweden

common hosts for producing plant secondary metabolites, such as resveratrol and vanillin-β-glucoside (Li et al. 2015; Liu et al. 2017; Strucko et al. 2015). Strucko et al. compared CEN.PK and S288c (parental strain of BY4741) for the production of vanillin glucoside, and found that the production of vanillin-β-glucoside in S288c was tenfold higher than that in CEN.PK under the continuous cultivation condition. Thus, we chose BY4741 as the host for optimizing L-tyrosine metabolic pathway in this study.

In *S. cerevisiae*, L-tyrosine synthesis starts with the shikimate pathway, a common pathway for synthesis of all three aromatic amino acids, which includes seven enzymatic reactions to synthesize chorismate (Braus 1991). First, one of the two 3-deoxy-D-arabino-heptulosonate-7-phosphate (DAHP) synthase isozymes, Aro3p and Aro4p, which are feedback-inhibited by L-phenylalanine and L-tyrosine, respectively, catalyzes the condensation of phosphoenolpyruvate (PEP) and erythrose 4-phosphate (E4P) to form DAHP (Paravicini et al. 1989). Then, DAHP is converted into 5-enolpyruvyl-shikimate-3-phosphate by a pentafunctional enzyme Aro1p, which catalyzes five reactions (Duncan et al. 1988; Graham et al. 1993). Finally, chorismate synthase Aro2p catalyzes the formation of chorismic acid, the last precursor common to all three aromatic amino acids (Braus 1991). Synthesis of prephenate (PPA), the last common precursor of both L-tyrosine and L-phenylalanine, is catalyzed by chorismate mutase Aro7p, whose activity is stimulated by L-tryptophan and inhibited by L-tyrosine (Hartmann et al. 2003; Luttik et al. 2008). Then, PPA is converted into *p*-hydroxyphenylpyruvate (HPP) by prephenate dehydrogenase Tyr1p, and L-tyrosine is obtained by reversible transamination of aromatic aminotransferase I Aro8p and aromatic aminotransferase II Aro9p (Iraqui et al. 1998; Karsten et al. 2011; Ohashi et al. 2017; Romagnoli et al. 2015). Meanwhile, HPP can also be converted into byproduct *p*-hydroxy-acetaldehyde by pyruvate decarboxylase Pdc5p or/and phenylpyruvate decarboxylase Aro10p (Fig. 1) (Choo et al. 2018; Vuralhan et al. 2005).

In the last decade, there have been several efforts to optimize L-tyrosine biosynthesis in *S. cerevisiae*, and research has generally focused on both eliminating the feedback inhibition of key enzymes and preventing the formation of byproducts. Overexpression of DAHP synthase gene $ARO4^{K229L}$ and chorismate mutase gene $ARO7^{G141S}$ could produce a 200-fold increase in extracellular aromatic amino acids compared to the reference strain and an increment of 4.5-fold of the flux through the aromatic amino acid biosynthesis pathway (Luttik et al. 2008). A triple knockout of the phenylpyruvate decarboxylase genes *ARO10*, *PDC5*, and *PDC6* could prevent the formation of byproduct phenylethanol, thus increasing the flux through the L-tyrosine biosynthesis pathway (Koopman et al. 2012). A *p*-coumaric acid overproducing platform strain was obtained by overexpressing feedback-resistant mutants of *ARO4* and *ARO7*, *E. coli* shikimate kinase II gene (*aro L*) and tyrosine ammonia-lyase (TAL) gene from *Flavobacterium johnsoniae* in a *Δpdc5Δaro10* background strain (Rodriguez et al. 2015). Gold et al. combined localized pathway engineering with global engineering of central metabolism to develop a strain that accumulated intracellular L-tyrosine up to 520 μmol g^{-1} dry cell weight or 192 mM in the cytosol (Gold et al. 2015).

Previous approaches to engineering L-tyrosine overproduction in *S. cerevisiae* were designed for only a few candidates of the L-tyrosine pathway at a time. Therefore, one pathway bottleneck might be eliminated using these approaches; while, another bottleneck might be introduced somewhere else within this pathway. In this study, we systematically analyzed nine genes necessary for production of L-tyrosine: seven for the L-tyrosine biosynthetic pathway and two for overproducing E4P and PEP. To facilitate the analysis of L-tyrosine and evaluate the strains as a platform for the synthesis of plant secondary metabolites derived from L-tyrosine, the TAL from *Rhodobacter capsulatus* was

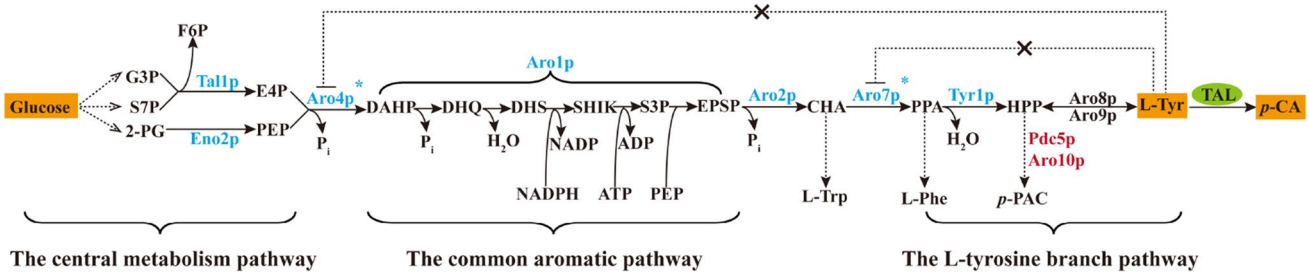

Fig. 1 Schematic illustration of the *p*-coumaric acid biosynthetic pathway in *S. cerevisiae*. *G3P* glyceraldehyde 3-phosphate, *S7P* sedoheptulose-7-phosphate, *2-PG* 2-phosphoglycerate, *F6P* fructose 6-phosphate, *E4P* erythrose 4-phosphate, *PEP* phosphoenolpyruvate, *DAHP* 3-deoxy-D-arabinoheptulosonic acid-7-phosphate, *DHQ* 3-dehydroquinate, *DHS* 3-dehydroshikimate, *SHIK* shikimate, *S3P* shikimate 3-phosphate, *EPSP* 5-enolpyruvyl-shikimate 3-phosphate, *CHA* chorismic acid, *PPA* prephenate, *HPP* *p*-hydroxyphenylpyruvate, *L-TRP* L-tryptophan, *L-PHE* L-phenylalanine, *L-TYR* L-tyrosine, *p-PAC* *p*-hydroxy-acetaldehyde, *TAL* tyrosine ammonia-lyase, *p-CA* *p*-coumaric acid. Genes in blue represent overexpression, while in red indicate deletion, the star represents allosteric regulation

employed to catalyze the conversion of L-tyrosine into *p*-coumaric acid (Kyndt et al. 2002). We modified not only the shikimate pathway but also the carbon flux to PEP and E4P. Our study provided a new strategy for the optimization of L-tyrosine metabolic pathway, obtained a L-tyrosine high-producing strain with inheritable stability and biosecurity, and developed a platform for the study of plant secondary metabolites deriving from L-tyrosine.

Materials and methods

Strains, plasmids, media, and growth conditions

All strains and plasmids used in this study are listed in Table 1.

Escherichia coli DH5α competent cells were purchased from ComWin Biotech Company (Beijing, China) and used for bacterial transformation and propagation. They were grown at 37 °C in Luria–Bertani broth (1% NaCl, 1% tryptone and 0.5% yeast extract) supplemented with ampicillin (100 mg L^{-1}) to select positive *E. coli* transformants (Liu et al. 2014).

Table 1 Strains and plasmids used

Strains and plasmids	Relevant characteristics	Source
E. coli strain		
E. coli DH5α	F-ϕ80d*lacZ*ΔM15 *endA1 recA1 hsd RI7*($r_K^- m_K^+$) *supE44 thi-1 relA1* Δ(*lacZYA-argF*)U169 *gyrA96 deoR*. Host strain to amplify plasmid DNA	Stratagene
S. cerevisiae strains		
BY4741	*MATa; his3Δ1; leu2Δ0; met15Δ0; ura3Δ0*	EUROSCARF, Frankfurt, Germany
NK-L71	BY4741; P_{GPD1}-*ENO2*; P_{GPD1}-*TAL1*	Mao et al. (2017)
NK-L107	NK-L71; P_{GPD1}-*ARO1*	Mao et al. (2017)
NKA2	NK-L107; P_{TEF1}-*ARO4*^{fbr}-T_{ADH1}	This study
NKA3	NK-L107; P_{PGK1}-*ARO7*^{fbr}-T_{CYC1}	This study
NKA4	NK-L107; P_{TEF1}-*ARO4*^{fbr}-T_{ADH1}; P_{PGK1}-*ARO7*^{fbr}-T_{CYC1}	This study
NKA5	NKA4; *pdc5*Δ::*loxP*	This study
NKA6	NKA4; *aro10*Δ::*loxP*	This study
NKA7	NKA4; *pdc5*Δ::*loxP*; *aro10*Δ::*loxP*	This study
NKA8	NKA7; P_{TEF1}-*TYR1*-T_{ADH1}	This study
NKA9	NKA7; P_{TEF1}-*ARO2*-T_{ADH1}	This study
BY4741T	BY4741; pLC-m7	This study
NK-L71T	NK-L71; pLC-m7	This study
NKA1T	NK-L107; pLC-m7	This study
NKA2T	NKA2; pLC-m7	This study
NKA3T	NKA3; pLC-m7	This study
NKA4T	NKA4; pLC-m7	This study
NKA5T	NKA5; pLC-m7	This study
NKA6T	NKA6; pLC-m7	This study
NKA7T	NKA7; pLC-m7	This study
NKA8T	NKA8; pLC-m7	This study
NKA9T	NKA9; pLC-m7	This study
Plasmids		
pUG72	Template for the *loxP-URA3-loxP* cassette, Amp^r	Hegemann and Heick (2011)
pSH62	*HIS3*, Cre expression vector	Hegemann and Heick (2011)
pLC41	2 μm ori, *HIS3*, P_{TEF1}-T_{ADH1}, P_{PGK1}-T_{CYC1}, Amp^r	This lab
pLC-m1	pSP-G1::P_{TEF1}-*ARO4*^{fbr}-T_{ADH1}, P_{PGK1}-*ARO7*^{fbr}-T_{CYC1}	Mao et al. (2017)
pLC-m2	pLC42::P_{TEF1}-*ARO2*-T_{ADH1}, P_{PGK1}-T_{CYC1}	Mao et al. (2017)
pLC-m3	pLC42::P_{TEF1}-*TYR1*-T_{ADH1}, P_{PGK1}-T_{CYC1}	Mao et al. (2017)
pLC-m7	pLC41::P_{TEF1}-T_{ADH1}, P_{PGK1}-*TAL*-T_{CYC1}	Mao et al. (2017)

Wild-type *S. cerevisiae* strain BY4741 (*MATa*; *his3Δ1*; *leu2Δ0*; *met15Δ0*; *ura3Δ0*) was obtained from Euroscarf (Frankfurt, Germany) and grown at 30 °C in synthetic complete (SC) medium (2% glucose, 0.67% yeast nitrogen base without amino acids and 0.13% amino acid mixture). Drop-out media (SC-Ura and SC-His), prepared using single drop-out mixture of amino acids (SD/ − uracil or SD/ − histidine), were used in the transformation and complementation experiments. The SG medium (2% galactose, 0.67% yeast nitrogen base without amino acids and 0.13% amino acid mixture) was used to induce expression of Cre recombinase in the yeast transformants. All solid media used in this study contained 2% agar.

For each engineered strain, three parallel correct transformants were picked and inoculated in 5 mL of SC-His liquid medium at 30 °C with 200-rpm agitation until cell density was saturated, and then cells were subcultured into 20 mL of SC-His medium in three 100-mL shaking flasks with a starting OD_{600} of 0.1. The cells in shaking flasks were cultivated at 30 °C and 200-rpm agitation for 120 h. Experimental samples were withdrawn every 12 h for OD_{600} measurements and product quantification.

Overexpression of *ARO4^{fbr}*, *ARO7^{fbr}*, *ARO2* and *TYR1*

The *ARO4^{fbr}* overexpression strain was constructed by replacing *ARO4* with the *URA3* and P_{TEF1}-*ARO4^{fbr}*-T_{ADH1} cassettes in strain NK-L107. A detailed overexpression route is illustrated in Fig. S1. The complete overexpression cassette was derived from four individual parts as follows. Part 1 consisted of a 679-bp upstream homologous sequence of *ARO4* and a 40–60-bp sequence homologous to the 5′-terminus of part 2. In part 2, a 40–60-bp sequence homologous to the 3′-terminus of part 1, the *URA3* cassette and a 40–60-bp sequence homologous to the 5′-terminus of part 3 were included. Part 3 comprised a 40–60-bp sequence homologous to the 3′-terminus of part 2, the P_{TEF1}-*ARO4^{fbr}*-T_{ADH1} cassette and a 40–60-bp sequence homologous to the 5′-terminus of part 4. In part 4, a 40–60-bp sequence homologous to the 3′-terminus of part 3 and a 660-bp downstream homologous sequence of *ARO4* were included.

The four parts were generated by PCR amplification using primers and templates listed in Table 2: *S. cerevisiae* genomic DNA was the PCR template of parts 1 and 4; plasmid pUG72 was used for amplifying part 2 (Hegemann and Heick 2011); and part 3 was amplified from plasmid pLC-m1 (Fig. S1) (Mao et al. 2017). After purification, the four parts were co-transformed into yeast strain utilizing a lithium acetate procedure described previously (Gietz and Woods 2002), and then the intact overexpression cassette was generated through recombination between the two 40 and 60-bp overlapping regions by means of the homologous recombination machinery of *S. cerevisiae*. More precisely, the upstream and downstream homologous sequences of parts 1 and 2 were used for targeted homologous recombination. Transformants were selected on SC-Ura yeast synthetic drop-out media and confirmed by PCR. The correct transformants were transformed with plasmid pSH62, and *URA3* selection marker was looped out by Cre recombinase expression induced by galactose (Hegemann and Heick 2011; Sauer 1987). The same method was used for overexpression of *ARO7^{fbr}*, *ARO2* and *TYR1*. The original genes *ARO7*, *ARO2* and *TYR1* were replaced by P_{PGK1}-*ARO7^{fbr}*-T_{CYC1}, P_{TEF1}-*ARO2*-T_{ADH1} and P_{TEF1}-*TYR1*-T_{ADH1} cassettes, amplified from plasmids pLC-m1, pLC-m2 and pLC-m3, respectively (Fig. S2) (Mao et al. 2017).

Deletion of *ARO10* and *PDC5*

The method of single gene deletion was similar to that of gene overexpression. The gene knockout cassette had three parts (Fig. S3). In part 1, a 600–1000-bp upstream homologous sequence of the target gene and a 40–60-bp sequence homologous to the 5′-terminus of part 2 were included. Part 2 consisted of a 40–60-bp sequence homologous to the 3′-terminus of part 1, the *URA3* cassette and a 40–60-bp sequence homologous to the 5′-terminus of part 3. Part 3 comprised a 40–60-bp sequence homologous to the 3′-terminus of part 2 and a 600–1000-bp downstream homologous sequence of the target gene. Parts 1 and 3 were amplified from *S. cerevisiae* genomic DNA, and plasmid pUG72 used as the PCR template for part 2 (Hegemann and Heick 2011). The three knockout fragments were transformed into *S. cerevisiae* and transformants were selected on SC-Ura yeast synthetic drop-out media. The target gene was replaced by a *URA3* cassette. Then, the Cre/lox P system was again used to remove the *URA3* cassette (Sauer 1987). All primers used are listed in Table 2. The double-deletion strain was obtained by sequential deletion of *PDC5* and *ARO10.*

Codon optimization, synthesis, and overexpression of *TAL*

The *TAL* from *R. capsulatus* was codon optimized and synthesized for *S. cerevisiae* by Genewiz (Su Zhou, China), assembled under *PGK1* promoter into pLC41 vector (Mao et al. 2017). The resulting plasmid named pLC-m7 was transformed into strain BY4741 and its derivative strains to generate a series of strains producing *p*-coumaric acid. Descriptions of strains and plasmids used in this study are summarized in Table 1.

Real time quantitative PCR (RT-PCR)

Strains were cultured at 30 °C in SC-His medium to exponential phase. The mRNAs were extracted using a RNApure

Table 2 Primers used

Primers	Sequences (5′-3′)	Applications
The overexpression of mutated DAHP synthase *ARO4* and chorismate mutase *ARO7* to avoid feedback inhibition		
1	CTGCACAACCCACATAATTC	Amplify *ARO4* upstream homologous region for $ARO4^{fbr}$ overexpression from *S. cerevisiae* genome, forward primer
2	CGACCTGCAGCGTACGAAGCTTCAGCTGGAGAGACT CTTCTAGTTATTCTTAATTAC	Amplify *ARO4* upstream homologous region for $ARO4^{fbr}$ overexpression from *S. cerevisiae* genome, reverse primer
3	GTAATTAAGAATAACTAGAAGAGTCTCTCCAGCTGA AGCTTCGTACGCTGCAGGTCG	Amplify *URA3* selection marker for $ARO4^{fbr}$ overexpression from pUG72, forward primer
4	CATCTTTGTAAAACTTCGATACCACACACGCGGCCG CATAGGCCACTAGTGGATCTG	Amplify *URA3* selection marker for $ARO4^{fbr}$ overexpression from pUG72, reverse primer, reverse primer
5	CAGATCCACTAGTGGCCTATGCGGCCGCGTGTGTGG TATCGAAGTTTTACAAAGATG	Amplify P_{TEF1}-$ARO4^{fbr}$-T_{ADH1} DNA fragment for $ARO4^{fbr}$ overexpression from pLC-m1, forward primer
6	CATCCACGAAATCAGTGAAAGGTCAGCGCACACACC ATAGCTTCAAAATGTTTCTAC	Amplify P_{TEF1}-$ARO4^{fbr}$-T_{ADH1} DNA fragment for $ARO4^{fbr}$ overexpression from pLC-m1, reverse primer
7	GTAGAAACATTTTGAAGCTATGGTGTGTGCGCTGAC CTTTCACTGATTTCGTGGATG	Amplify *ARO4* downstream homologous region for $ARO4^{fbr}$ overexpression from *S. cerevisiae* genome, forward primer
8	CCTATTTCTGGTACTGGCTTTTC	Amplify *ARO4* downstream homologous region for $ARO4^{fbr}$ overexpression from *S. cerevisiae* genome, reverse primer
9	GATCGTATATGACACAACGAGG	Amplify *ARO7* upstream homologous region for $ARO7^{fbr}$ overexpression from *S. cerevisiae* genome, forward primer
10	CGACCTGCAGCGTACGAAGCTTCAGCTGATCTTATA CCAATTTTATGCAGGATGCTG	Amplify *ARO7* upstream homologous region for $ARO7^{fbr}$ overexpression from *S. cerevisiae* genome, reverse primer
11	CAGCATCCTGCATAAAATTGGTATAAGATCAGCTGA AGCTTCGTACGCTGCAGGTCG	Amplify *URA3* selection marker for $ARO7^{fbr}$ overexpression from pUG72, forward primer
12	GATAAGACCCCATTCTTTGAAGGTACTTCCCGGCCG CATAGGCCACTAGTGGATCTG	Amplify *URA3* selection marker for $ARO7^{fbr}$ overexpression from pUG72, reverse primer, reverse primer
13	CAGATCCACTAGTGGCCTATGCGGCCGGGAAGTACC TTCAAAGAATGGGGTCTTATC	Amplify P_{PGK1}-$ARO7^{fbr}$-T_{CYC1} DNA fragment for $ARO7^{fbr}$ overexpression from pLC-m1, forward primer
14	GTGGAATTGTTACCGTGATAGCCTTCATGCCTTCGA GCGTCCCAAAACCTTCTCAAGC	Amplify P_{PGK1}-$ARO7^{fbr}$-T_{CYC1} DNA fragment for $ARO7^{fbr}$ overexpression from pLC-m1, reverse primer
15	GCTTGAGAAGGTTTTGGGACGCTCGAAGGCATGAAG GCTATCACGGTAACAATTCCAC	Amplify *ARO7* downstream homologous region for $ARO7^{fbr}$ overexpression from *S. cerevisiae* genome, forward primer
16	GTCATCGACTTTGTCATTGCC	Amplify *ARO7* downstream homologous region for $ARO7^{fbr}$ overexpression from *S. cerevisiae* genome, reverse primer
The knockout of *ARO10* (phenylpyruvate decarboxylase) and *PDC5* (pyruvate decarboxylase) to avoid production of aromatic alcohols and direct the pathway flux to aromatic amino acids		
17	CCTCTTCTTCTTGTGTGTTTAAGC	Amplify *ARO10* upstream homologous region for *ARO10* knockout from *S. cerevisiae* genome, forward primer
18	CGACCTGCAGCGTACGAAGCTTCAGCTGGCTTAAGG GAGTTTCTTTGTTATCTTG	Amplify *ARO10* upstream homologous region for *ARO10* knockout from *S. cerevisiae* genome, reverse primer
19	CAAGATAACAAAGAAACTCCCTTAAGCCAGCTGAAG CTTCGTACGCTGCAGGTCG	Amplify *URA3* selection marker for *ARO10* knockout from pUG72, forward primer

Table 2 (continued)

Primers	Sequences (5′-3′)	Applications
20	CACACGATAGGAATGACAGAAAAAAGCGGCCGCATAGGCCACTAGTGGATCTG	Amplify *URA3* selection marker for *ARO10* knockout from pUG72, reverse primer
21	CAGATCCACTAGTGGCCTATGCGGCCGCTTTTTTCTGTCATTCCTATCGTGTG	Amplify *ARO10* downstream homologous region for *ARO10* knockout from *S. cerevisiae* genome, forward primer
22	CGAAGTATTTCGGACTCTTTCTTC	Amplify *ARO10* downstream homologous region for *ARO10* knockout from *S. cerevisiae* genome, reverse primer
23	GTTGAAAATGACGACGAGCCTG	Amplify *PDC5* upstream homologous region for *PDC5* knockout from *S. cerevisiae* genome, forward primer
24	CGACCTGCAGCGTACGAAGCTTCAGCTGGTGTAATAAGAAAGAGAGGAAAGGAC	Amplify *PDC5* upstream homologous region for *PDC5* knockout from *S. cerevisiae* genome, reverse primer
25	GTCCTTTCCTCTCTTTCTTATTACACCAGCTGAAGCTTCGTACGCTGCAGGTCG	Amplify *URA3* selection marker for *PDC5* knockout from pUG72, forward primer
26	CCTAAACATCTATAACCTTCAAAAGCGGCCGCATAGGCCACTAGTGGATCTG	Amplify *URA3* selection marker for *PDC5* knockout from pUG72, reverse primer
27	CAGATCCACTAGTGGCCTATGCGGCCGCTTTTGAAGGTTATAGATGTTTAGG	Amplify *PDC5* downstream homologous region for *PDC5* knockout from *S. cerevisiae* genome, forward primer
28	CTCTTGCTTGTTCGGAGTTC	Amplify *PDC5* downstream homologous region for *PDC5* knockout from *S. cerevisiae* genome, reverse primer
Overexpression of L-tyrosine pathway genes *ARO2* and *TYR1*		
29	CGTGAACACGTACACTATACG	Amplify *ARO2* upstream homologous region for *ARO2* overexpression from *S. cerevisiae* genome, forward primer
30	CGACCTGCAGCGTACGAAGCTTCAGCTGCGATGAGAATAACGCTTAGATGATGCCG	Amplify *ARO2* upstream homologous region for *ARO2* overexpression from *S. cerevisiae* genome, reverse primer
31	CGGCATCATCTAAGCGTTATTCTCATCGCAGCTGAAGCTTCGTACGCTGCAGGTCG	Amplify *URA3* selection marker for *ARO2* overexpression from pUG72, forward primer
32	CATCTTTGTAAAACTTCGATACCACACACGCGGCCGCATAGGCCACTAGTGGATCTG	Amplify *URA3* selection marker for *ARO2* overexpression from pUG72, reverse primer, reverse primer
33	CAGATCCACTAGTGGCCTATGCGGCCGCGTGTGTGGTATCGAAGTTTTACAAAGATG	Amplify P_{TEF1}-*ARO2*-T_{ADH1} DNA fragment for *ARO2* overexpression from pLC-m2, forward primer
34	CATAACTCTTGAGGGGTTTTGTTTCTATCGCACACACCATAGCTTCAAAATGTTTCTAC	Amplify P_{TEF1}-*ARO2*-T_{ADH1} DNA fragment for *ARO2* overexpression from pLC-m2, reverse primer
35	GTAGAAACATTTTGAAGCTATGGTGTGTGCGATAGAAACAAAACCCCTCAAGAGTTATG	Amplify *ARO2* downstream homologous region for *ARO2* overexpression from *S. cerevisiae* genome, forward primer
36	CATTGATGTTACCTTCACCAAGG	Amplify *ARO2* downstream homologous region for *ARO2* overexpression from *S. cerevisiae* genome, reverse primer
37	CCCATCTTTGAAAACTCTAACG	Amplify *TYR1* upstream homologous region for *TYR1* overexpression from *S. cerevisiae* genome, forward primer
38	CGACCTGCAGCGTACGAAGCTTCAGCTGGTTTATCAAGTGGATATGCTGTCCTCTTTC	Amplify *TYR1* upstream homologous region for *TYR1* overexpression from *S. cerevisiae* genome, reverse primer

Table 2 (continued)

Primers	Sequences (5′-3′)	Applications
39	GAAAGAGGACAGCATATCCACTTGATAAACCAGCTG AAGCTTCGTACGCTGCAGGTCG	Amplify *URA3* selection marker for *TYR1* overexpression from pUG72, forward primer
40	CATCTTTGTAAAACTTCGATACCACACACGCGGCCG CATAGGCCACTAGTGGATCTG	Amplify *URA3* selection marker for *TYR1* overexpression from pUG72, reverse primer, reverse primer
41	CAGATCCACTAGTGGCCTATGCGGCCGCGTGTGTGG TATCGAAGTTTTACAAAGATG	Amplify P_{TEF1}-*TYR1*-T_{ADH1} DNA fragment for *TYR1* overexpression from pLC-m3, forward primer
42	CGATAATCGCGGTAGTGAGCATTACACGCACACACC ATAGCTTCAAAATGTTTCTAC	Amplify P_{TEF1}-*TYR1*-T_{ADH1} DNA fragment for *TYR1* overexpression from pLC-m3, reverse primer
43	GTAGAAACATTTTGAAGCTATGGTGTGTGCGTGTAA TGCTCACTACCGCGATTATCG	Amplify *TYR1* downstream homologous region for *TYR1* overexpression from *S. cerevisiae* genome, forward primer
44	CGACCAGGATCCATATATC	Amplify *TYR1* downstream homologous region for *TYR1* overexpression from *S. cerevisiae* genome, reverse primer
Quantitative real-time PCR		
45	GTGAACAATTACACAGCTCCTATAG	Amplify partial cDNA of *S. cerevisiae ALG9* gene for real-time PCR, forward primer
46	CCTATGATTATCTGGCAGCAGGAAAG	Amplify partial cDNA of *S. cerevisiae ALG9* gene for real-time PCR, reverse primer
47	CTGGTGATTTCGGCTCTATTGCCAAG	Amplify partial cDNA of *S. cerevisiae TAL1* gene for real-time PCR, forward primer
48	GGTGGTCTTACCATGCTTCTTACCG	Amplify partial cDNA of *S. cerevisiae TAL1* gene for real-time PCR, reverse primer
49	GACTTGTCTAAGTCCAAGACCTCTCC	Amplify partial cDNA of *S. cerevisiae ENO2* gene for real-time PCR, forward primer
50	CATGGCTTCAGCGAAGGTCTTAGC	Amplify partial cDNA of *S. cerevisiae ENO2* gene for real-time PCR, reverse primer
51	CCTGGAATTCAAGGCTTCTTTGCCAG	Amplify partial cDNA of *S. cerevisiae ARO1* gene for real-time PCR, forward primer
52	CGCTACCATAACCGTATCACGAGTAC	Amplify partial cDNA of *S. cerevisiae ARO1* gene for real-time PCR, reverse primer
53	CGCTAACGGTGAAAACGCCATTACC	Amplify partial cDNA of *S. cerevisiae ARO4* gene for real-time PCR, forward primer
54	CGTCTTCAGTAGTTTCCCAACCTATAC	Amplify partial cDNA of *S. cerevisiae ARO4* gene for real-time PCR, reverse primer
55	GAGAGGTCGCATTTCGCCACATG	Amplify partial cDNA of *S. cerevisiae ARO7* gene for real-time PCR, forward primer
56	CAGGTGATTCGAATCTTCTGATGCG	Amplify partial cDNA of *S. cerevisiae ARO7* gene for real-time PCR, reverse primer
57	GGTCATTTGGTATCCAGGCAAAGCG	Amplify partial cDNA of *S. cerevisiae TYR1* gene for real-time PCR, forward primer

Table 2 (continued)

Primers	Sequences (5′-3′)	Applications
58	CTCGATTTCCGGCAGCTTACAACTC	Amplify partial cDNA of *S. cerevisiae TYR1* gene for real-time PCR, reverse primer
59	GCTTCAGGTGCCATTGCTGAGAAG	Amplify partial cDNA of *S. cerevisiae ARO2* gene for real-time PCR, forward primer
60	CCTGGTGATGGTGTTCAACAGATGC	Amplify partial cDNA of *S. cerevisiae ARO2* gene for real-time PCR, reverse primer

yeast kit (CWBIO, Beijing, China) and reverse transcribed into cDNAs using a superRT cDNA kit (CWBIO). The gene relative expression levels were quantified by RT-qPCR using Hieff™ qPCR SYBR green master mix (Yeasen, Shanghai, China). The gene *ALG9*, which had a relatively stable expression level, was used as the reference gene. All of the primers used are listed in Table 2 and the data were analyzed using threshold cycle ($2^{-\Delta\Delta CT}$) method. Each experiment was performed in triplicate.

High-performance liquid chromatograph (HPLC) analysis of products

Samples were centrifuged at 12,000*g* for 5 min and the supernatant was extracted and filtered through 0.22-μm pore-size polyethersulfone membrane syringe filters for HPLC analysis.

For quantification of *p*-coumaric acid, a HPLC coupled with an ultraviolet detector and an inertsil ODS-3/C18 column (250 mm × 4.6 mm, 5 μm) was used. Mobile phases A and B were composed of water (5% acetonitrile and 0.1% trifluoroacetic acid) and acetonitrile (0.1% trifluoroacetic acid), respectively. A gradient method was used with a flow rate of 1 mL min^{-1}: 6–50% phase B for 15 min, 50–98% phase B for 15 min, 98% phase B for 3 min, 98–6% for 2 min and 6% phase B for an additional 5 min. The injection volume was 10 μL. Quantification was based on the peak areas of absorbance at 310 nm and retention time was 16.9 min.

Glucose was analyzed by a Waters Alliance 2695 HPLC (Waters, Milford, MA, USA) equipped with an isocratic pump, a refractive index detector and a Hitachi auto sampler. A Bio-Rad Aminex HPX-87H column (300 × 7.8 mm) was utilized at 65 °C with 5 mM H_2SO_4 as the mobile phase at a flow rate of 0.6 m L min^{-1}.

Statistical analysis

Data were expressed as means ± standard errors. Student's *t* test was used to compare the difference between engineered and parental strains. Statistical significance was $p < 0.05$.

Results

Effects of overexpression of enolase II, transaldolase, and pentafunctional enzyme Aro1p on *p*-coumaric acid production

Both E4P and PEP are the intermediate metabolites of the pentose phosphate and glycolytic pathways, respectively (Fig. 1). To enhance the supply of E4P and PEP, the transaldolase, which catalyzes conversion of sedoheptulose-7-phosphate and glyceraldehyde 3-phosphate into E4P and

fructose 6-phosphate, and enolase II, which catalyzes the conversion of 2-phosphoglycerate into PEP, were simultaneously overexpressed through promoter replacement in situ in wild-type *S. cerevisiae* BY4741, generating the engineered strain NK-L71. Their original promoter was replaced by a strong *GPD1* promoter, which was previously described by Mao et al. (2017). The promoter of Aro1p was also replaced by *GPD1* promoter in the strain NK-L71 to yield an engineered strain NK-L107 (Fig. 2). Furthermore, *p*-coumaric acid production strains NK-L71T and NKA1T were constructed by introducing pLC-m7 into strains NK-L71 and NK-L107, respectively.

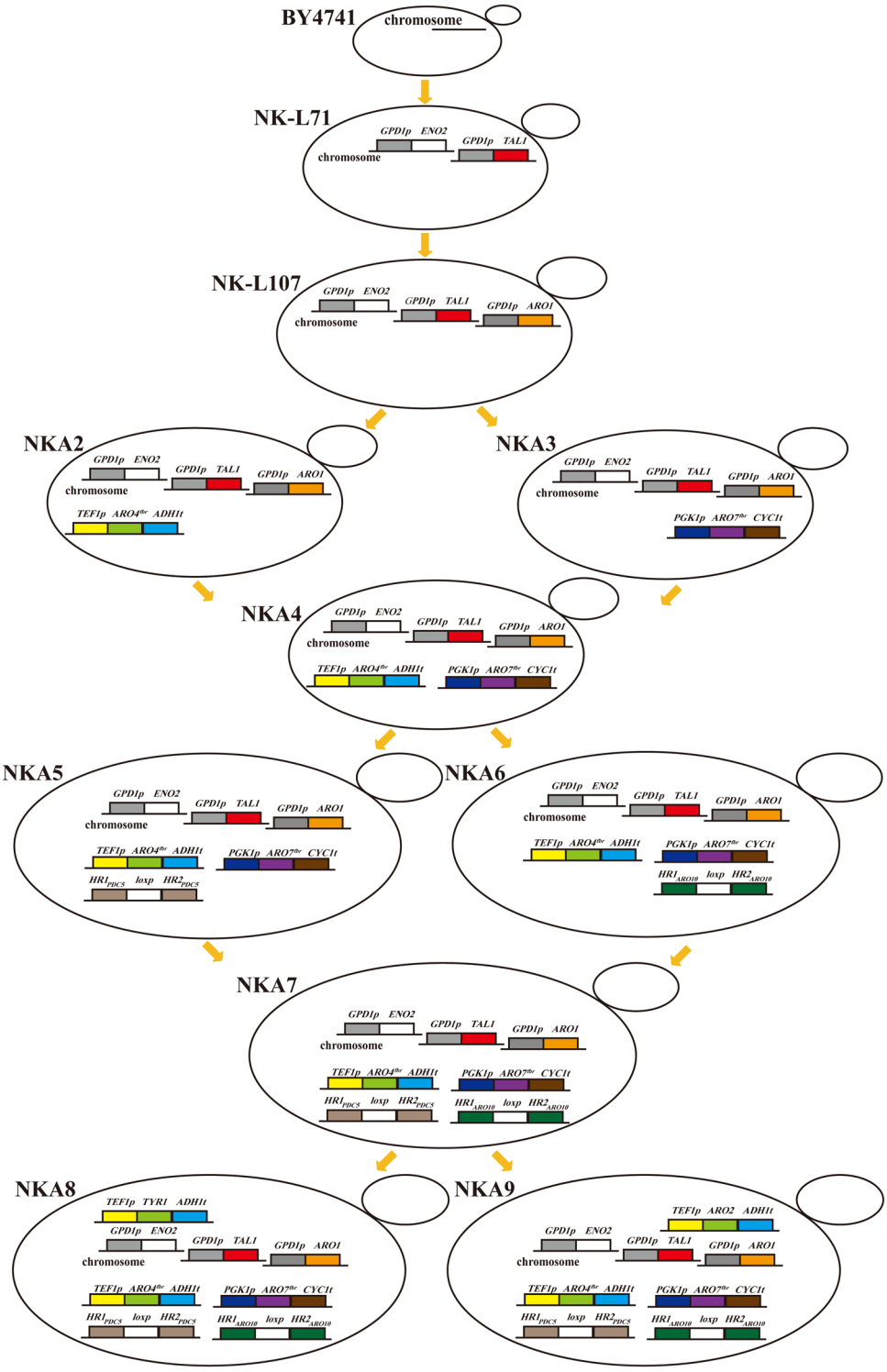

Fig. 2 Schematic representation of the engineered strains NK-L71, NK-L107, NKA2, NKA3, NKA4, NKA5, NKA6, NKA7, NKA8 and NKA9. Promoters of *TAL1*, *ENO2*, and *ARO1* were replaced with a strong constitutive promoter P_{GPD1}; $ARO4^{K229L}$ was overexpressed under the strong constitutive promoter P_{TEF1} at the *ARO4* locus; $ARO7^{G141S}$ was overexpressed under the strong constitutive promoter P_{PGK1} at the *ARO7* locus; *TYR1* and *ARO2* were overexpressed under the strong constitutive promoter P_{TEF1} in situ, respectively

The RT-qPCR analysis indicated that replacement of the promoter could significantly up-regulate the gene expression levels (Fig. 3). Fermentations were performed and *p*-coumaric acid production was determined daily—peaking at 48 h and then decreasing gradually (Fig. S4). The reference strain BY4741T produced 1.40 mg L^{-1} of *p*-coumaric acid; the engineered strain NK-L71T overexpressing *ENO2* and *TAL1* produced 1.81 mg L^{-1}; and the engineered strain NKA1T overexpressing *ENO2*, *TAL1* and *ARO1* increased *p*-coumaric acid production to 2.17 mg L^{-1}, which was 1.55-fold higher than that of the reference strain (Fig. 4). Thus, enhancing supply of E4P and PEP, and overexpression of Aro1p, had a positive effect on production of *p*-coumaric acid. There were no significant differences in growth rates and glucose consumption rates between the reference strain and engineered strains (Figs. S5 and S6).

p-Coumaric acid production after overexpression of feedback-resistant mutants of DAHP synthase and chorismate mutase

DAHP synthase, encoded by *ARO4*, and chorismate mutase, encoded by *ARO7*, are both feedback inhibited by L-tyrosine. Substitution of the lysine residue 229 by a leucine relieved the inhibiting effect of L-tyrosine, leading to a feedback-resistant DAHP synthase. A single serine-to-glycine substitution in Aro7p at position 114 resulted in a feedback-resistant chorismate mutase (Luttik et al. 2008). To increase the activity of Aro4p and Aro7p, we performed single overexpression of mutated feedback-resistant $ARO4^{K229L}$, $ARO7^{G141S}$, and simultaneous overexpression of $ARO4^{K229L}$ and $ARO7^{G141S}$ in background strain NK-L107, resulting in strains NKA2, NKA3, and NKA4, respectively (Fig. 2). By introducing plasmid pLC-m7 into strains NKA2, NKA3, and NKA4, respectively, we obtained three *p*-coumaric acid production strains NKA2T, NKA3T, and NKA4T.

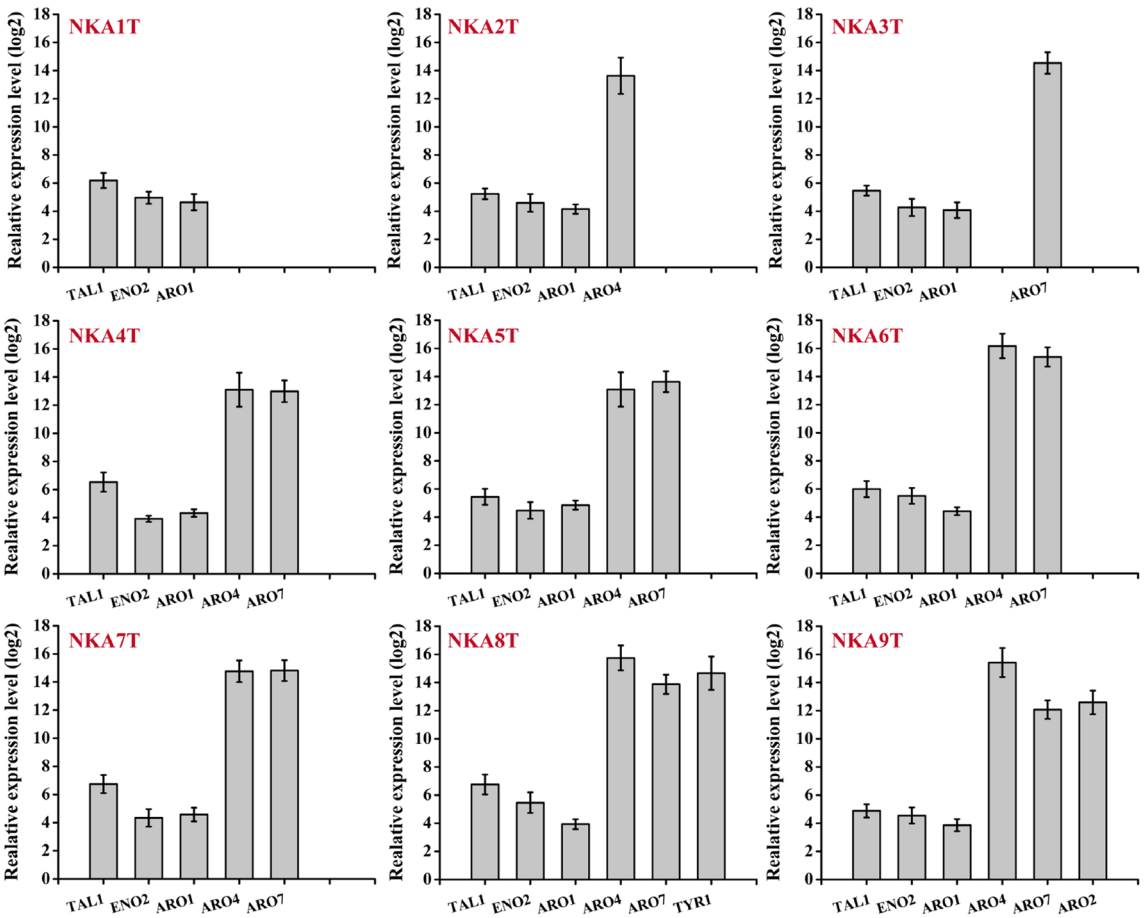

Fig. 3 The RT-qPCR analysis of gene expression levels of the engineered strains compared with BY4741T strain. Average ± standard deviations were calculated from three biological replicates. mRNAs were extracted using a RNApure yeast kit (CWBIO, Beijing, China) and reverse transcribed into cDNAs using a superRT cDNA kit (CWBIO). The gene relative expression levels were quantified by RT-qPCR using Hieff™ qPCR SYBR green master mix (Yeasen, Shanghai, China). The gene *ALG9* was used as the reference gene. Data were analyzed using threshold cycle ($2^{-\Delta\Delta CT}$) method

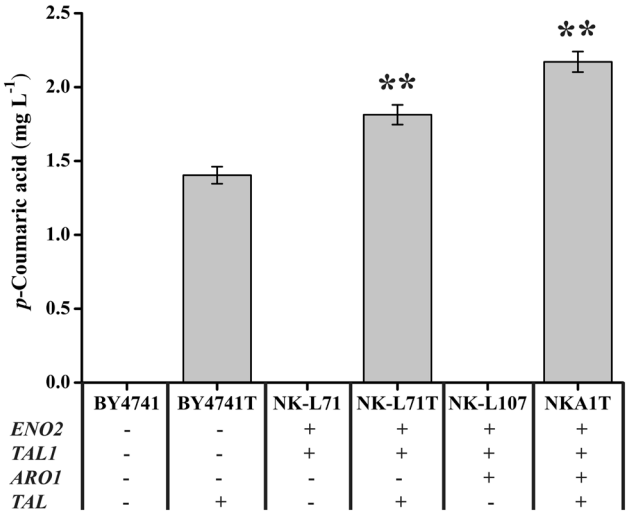

Fig. 4 Effect of the overexpression of *ENO2*, *TAL1*, and *ARO1* on *p*-coumaric acid production in strains overexpressing tyrosine ammonia-lyase *RcTAL* from *Rhodobacter capsulatus*. Strains were cultured in 20 mL of SC-His medium at 30 °C and 200 rpm, and *p*-coumaric acid production peaked at 48 h. Average ± standard deviations were calculated from three biological replicates. *$p < 0.05$, **$p < 0.01$ represent statistical significance compared with the BY4741T strain

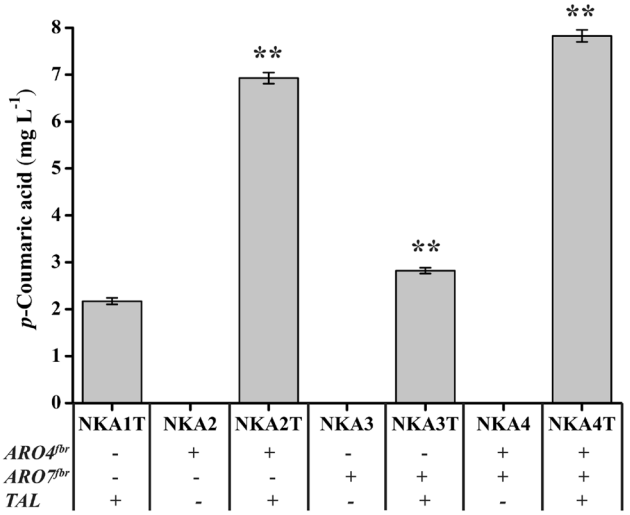

Fig. 5 Production of *p*-coumaric acid upon overexpression of $ARO4^{fbr}$ and $ARO7^{fbr}$ in strains with overexpression of *ENO2*, *TAL1*, *ARO1* and *RcTAL*. Strains were cultured in 20 mL of SC-His medium at 30 °C and 200 rpm. *p*-Coumaric acid of NKA1T strain peaked at 48 h and of NKA2T, NKA3T, and NKA4 peaked at 120 h. Average ± standard deviations were calculated from three biological replicates. *$p < 0.05$, **$p < 0.01$ represent statistical significance compared with the NKA1T strain

After confirmation of gene expressions by RT-qPCR (Fig. 3), fermentations were performed. Unlike the reference strain NKA1T, the *p*-coumaric acid production of all three engineered strains peaked at 120 h (Fig. S4). The strain NKA2T with single overexpression of $ARO4^{K229L}$ produced 6.93 mg L^{-1} of *p*-coumaric acid, but the strain NKA3T with overexpression of $ARO7^{G141S}$ produced 2.82 mg L^{-1}. The highest production (7.83 mg L^{-1}) was achieved in the strain NKA4T with the combined overexpression of $ARO4^{K229L}$ and $ARO7^{G141S}$ (Fig. 5). These results showed that elimination of feedback inhibition had a positive effect on *p*-coumaric acid production, and co-expression of $ARO4^{K229L}$ and $ARO7^{G141S}$ enhanced the yield further. The engineered strains showed a slower growth rate and lower glucose consumption compared with the control strain (Figs. S5 and S6).

Effect of elimination of competing phenylpyruvate decarboxylase activity on *p*-coumaric acid production

To reduce the diversion of carbon flux into the Ehrlich pathway, and further improve *p*-coumaric acid production, the *PDC5* and *ARO10* were deleted in background strain NKA4, generating the *PDC5* knockout strain NKA5, *ARO10* knockout strain NKA6, and double-knockout strain NKA7 (Δ*pdc5* and Δ*aro10*) (Fig. 2). The three engineered strains were transformed with plasmid pLC-m7, resulting in three *p*-coumaric acid production strains NKA5T, NKA6T, and NKA7T, respectively.

All three *p*-coumaric acid production strains had the highest production at 120 h (Fig. S4). The *p*-coumaric acid production of single-deletion strains NKA5T and NKA6T increased to 11.75 and 13.10 mg L^{-1}, respectively, and were correspondingly 1.50- and 1.67-fold higher than that of the control strain NKA4T. The double deletion of *PDC5* and *ARO10* resulted in the highest production (19.71 mg L^{-1}), indicating that deletion of the two phenylpyruvate decarboxylase genes *PDC5* and *ARO10* had a synergetic relationship in improving *p*-coumaric acid production (Fig. 6). A slight reduction of growth rate and glucose consumption occurred in the engineered strains (Figs. S5 and S6).

Overexpression of chorismate synthase and prephenate dehydrogenase

To find flux-controlling steps and further improve *p*-coumaric acid production, *TYR1* (prephenate dehydrogenase) and *ARO2* (chorismate synthase) were separately overexpressed in background strain NKA7 to yield strains NKA8 and NKA9, accordingly (Fig. 2). Then, plasmid pLC-m7 was transformed into these two strains, generating *p*-coumaric acid production strains NKA8T and NKA9T. The RT-qPCR assay revealed that the expression levels of *ARO2* and *TYR1* were significantly improved through genetic modification. However, overexpression of these two enzymes resulted in lower *p*-coumaric acid production than in the control strain (Fig. 7).

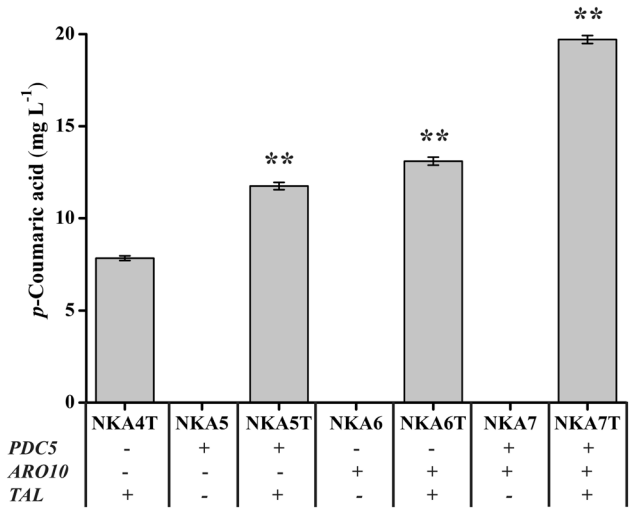

Fig. 6 Production of *p*-coumaric acid upon deletion of *PDC5* and *ARO10* in strains with overexpression of *ENO2*, *TAL1*, *ARO1*, $ARO4^{fbr}$, $ARO7^{fbr}$ and *RcTAL*. Strains were cultured in 20 mL of SC-His medium at 30 °C and 200 rpm, and *p*-coumaric acid production peaked at 120 h. Average ± standard deviations were calculated from three biological replicates. $*p < 0.05$, $**p < 0.01$ represent statistical significance compared with the NKA4T strain

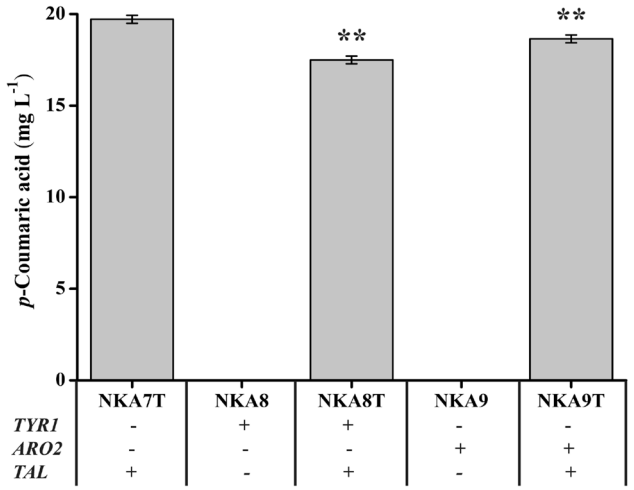

Fig. 7 Effect of overexpression of *TYR1* or *ARO2* on *p*-coumaric acid production in strains overexpressing *ENO2*, *TAL1*, *ARO1*, $ARO4^{fbr}$, $ARO7^{fbr}$, and *RcTAL* and deletion of *PDC5* and *ARO10*. Strains were cultured in 20 mL of SC-His medium at 30 °C and 200 rpm, and *p*-coumaric acid production peaked at 120 h. Average ± standard deviations were calculated from three biological replicates. $*p < 0.05$, $**p < 0.01$ represent statistical significance compared with the NKA7T strain

Comparison of *p*-coumaric acid highest-producing strain and wild-type strain

Through optimization of the L-tyrosine pathway above, we obtained strain NKA7T, which was the highest producer of *p*-coumaric acid. Strain NKA7T had a slightly reduced growth rate in 48 h, but the final OD value of NKA7T was a little higher than that of BY4741T (Fig. 8a). The glucose consumption of NKA7T was slightly lower than that of BY4741T in 12 h and glucose was entirely consumed after 24 h in the fermentation process of NKA7T and BY4741T (Fig. 8b). Production of *p*-coumaric acid was determined daily, and peaked at 48 h in BY4741T; however, *p*-coumaric acid concentration kept increasing until day 120 h for NKA7T (Fig. 8c). The *p*-coumaric acid production of NKA7T reached 19.71 mg L^{-1}, which was 14.08-fold higher than that of the wild-type BY4741T.

Discussion

We performed a series of genetic modifications to wild-type *S. cerevisiae* strain BY4741 to direct the carbon flux to L-tyrosine, and then introduced the heterologous TAL as a test of the metabolic engineering targets for improving carbon flux through the L-tyrosine pathway and the strain's ability to synthesize heterologous metabolites derived from L-tyrosine. Meanwhile, the effect of optimizing L-tyrosine metabolic pathway on strain growth and glucose consumption was analyzed.

The carbon flux to E4P and PEP was optimized by overexpressing *TAL1* and *ENO2*, respectively, and a 1.29-fold improvement of *p*-coumaric acid was obtained. Overexpression of *ARO1* was effective in increasing *p*-coumaric acid production. This is consistent with the results of Rodriguez et al., in which *p*-coumaric acid production increased significantly with overexpression of *ARO1* (Rodriguez et al. 2015). The overexpression of feedback-resistant $ARO4^{K229L}$ and $ARO7^{G141S}$ had a positive effect on *p*-coumaric acid production. The overexpression of $ARO4^{K229L}$ led to a 3.19-fold improvement compared to the control strain, but only 1.30-fold production was achieved by overexpressing $ARO7^{G141S}$. This was expected, because overexpression of feedback-resistant mutant of DAHP synthase was previously reported to have a greater effect on L-tyrosine yield than overexpression of feedback-resistant mutant of chorismate mutase (Luttik et al. 2008). Koopman et al. reported that eliminating feedback inhibition not only increased the production of naringenin, a derivative of L-tyrosine, but also led to increased phenylethanol production, the major byproduct of L-tyrosine biosynthesis (Koopman et al. 2012). Therefore, we made the double deletion of *PDC5* and *ARO10*, and this resulted in strongly increased *p*-coumaric acid production. This is also supported by research of Koopman et al., who significantly improved production of naringenin by a triple deletion of phenylpyruvate decarboxylases (Koopman et al. 2012).

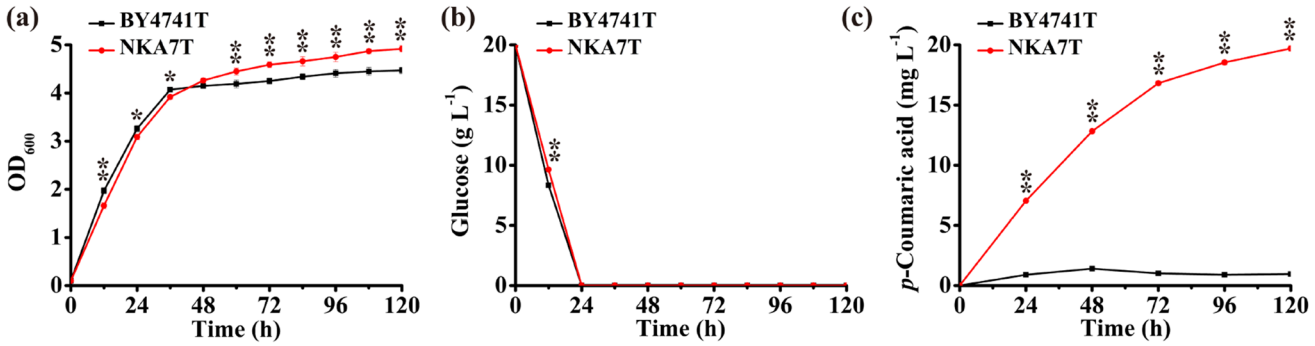

Fig. 8 The comparison of wild-type strain and *p*-coumaric acid highest-producing strain. Strains were cultured in 20 mL of SC-His medium at 30 °C and 200 rpm for 5 days: **a** cell growth, **b** glucose consumption, and **c** formation of *p*-coumaric acid. Average ± standard deviations were calculated from three biological replicates. $*p < 0.05$, $**p < 0.01$ represent statistical significance

The purpose of our study was the optimization of the L-tyrosine metabolic pathway in *S. cerevisiae*. We optimized the shikimate pathway and the carbon flux to E4P and PEP. The simultaneous overexpression of $ARO4^{K229L}$ and $ARO7^{G141S}$ led to a 3.61-fold improvement in *p*-coumaric acid production, but the same genetic modification by Rodriguez et al. only led to a 1.93-fold improvement (Rodriguez et al. 2015). Production of *p*-coumaric acid with double deletion of *PDC5* and *ARO10* showed a 2.52-fold increase in our study, which was higher than the 2.29-fold improvement reported by Rodriguez et al. when using the same genetic modification. Moreover, optimization of the L-tyrosine metabolic pathway in our research finally led to a 14.08-fold increase in *p*-coumaric acid, which was also higher than 7.90-fold reported by Rodriguez et al. These results might be due to the overexpression of *TAL1* and *ENO2* in our research, which increased the carbon flux to E4P and PEP, respectively.

The overexpression of *TYR1* had a negative effect on *p*-coumaric acid production, which coincided with the result of Rodriguez et al. (Rodriguez et al. 2015). They also reported that overexpression of *ARO1* could significantly improve *p*-coumaric acid production, but the *p*-coumaric acid titer of a strain simultaneously overexpressing *ARO1* and *ARO2* was very similar to that of the strain overexpressing *ARO1* alone (Rodriguez et al. 2015). In our research, the combined overexpression of *ARO1* and *ARO2* produced less *p*-coumaric acid compared with the strain overexpressing *ARO1* alone, which was not consistent with the result of Rodriguez et al. This result may be due to the different background strains we used compared with Rodriguez et al., and, in addition, the two strains were also modified differently. Our background strain was *S. cerevisiae* BY4741 and the modified strain before *ARO2* overexpression was NKA7. However, the background strain used by Rodriguez et al. was *S. cerevisiae* CEN.PK102-5B and the modified strain was ST3213 (*aro10*Δ *pdc5*Δ $ARO4^{K229L}$ $ARO7^{G141S}$). The reduction of *p*-coumaric acid production indicated that these two enzymes may not be bottlenecks for the L-tyrosine biosynthesis pathway in the engineered strain NKA7T; consequently, there may be other bottlenecks in the L-tyrosine pathway.

In conclusion, by optimizing supply of precursors, eliminating feedback inhibition and decreasing production of L-tyrosine byproducts, we obtained a series of strains producing *p*-coumaric acid. Among these strains, NKA7T was the highest producing, and the titer was 14.08-fold higher than that of the BY4741T (Fig. S7). The growth rate and glucose uptake rate of NKA7T showed only slight decreases compared with the wild-type strain. All of the genetic modifications of the L-tyrosine pathway were carried on chromosomes to ensure genetic stability, and selection marker gene was removed using the Cre/lox P system to ensure biosecurity, making this a good platform strain to produce L-tyrosine and research secondary metabolites derived from L-tyrosine.

Acknowledgements This work was supported by the Tianjin Key Research Program of Application Foundation and Advanced Technology [17JCZDJC32200]; the National Natural Science Foundation of China [31770102]; the Sino-Swiss Scientific and Technological Cooperation Project supported by the Ministry of Science and Technology of China [2015DFG32140].

Author contributions All authors contributed to the conception and design of the study, performing experimental assessments, drafting the articles, and revising it. All authors have contributed, seen and approved the manuscript.

Compliance with ethical standards

Conflict of interest The authors declare that they have no conflict of interest.

References

Akinwumi BC, Bordun KAM, Anderson HD (2018) Biological activities of stilbenoids. Int J Mol Sci 19(3):792. https://doi.org/10.3390/Ijms19030792

Borodina I, Nielsen J (2014) Advances in metabolic engineering of yeast *Saccharomyces cerevisiae* for production of chemicals. Biotechnol J 9(5):609–620. https://doi.org/10.1002/biot.201300445

Braus GH (1991) Aromatic amino acid biosynthesis in the yeast *Saccharomyces cerevisiae*: a model system for the regulation of a eukaryotic biosynthetic pathway. Microbiol Rev 55(3):349–370

Choo JH, Han C, Lee DW, Sim GH, Moon HY, Kim JY, Song JY, Kang HA (2018) Molecular and functional characterization of two pyruvate decarboxylase genes, *PDC1* and *PDC5*, in the thermotolerant yeast *Kluyveromyces marxianus*. Appl Microbiol Biotechnol 102(8):3723–3737. https://doi.org/10.1007/s00253-018-8862-3

Chougule M, Patel AR, Sachdeva P, Jackson T, Singh M (2011) Anticancer activity of Noscapine, an opioid alkaloid in combination with Cisplatin in human non-small cell lung cancer. Lung Cancer 71(3):271–282. https://doi.org/10.1016/j.lungcan.2010.06.002

Donnez D, Jeandet P, Clement C, Courot E (2009) Bioproduction of resveratrol and stilbene derivatives by plant cells and microorganisms. Trends Biotechnol 27(12):706–713. https://doi.org/10.1016/j.tibtech.2009.09.005

Duncan K, Edwards RM, Coggins JR (1988) The *Saccharomyces cerevisiae* ARO1 gene. An example of the co-ordinate regulation of five enzymes on a single biosynthetic pathway. FEBS Lett 241(1–2):83–88

Gietz RD, Woods RA (2002) Transformation of yeast by lithium acetate/single-stranded carrier DNA/polyethylene glycol method. Method Enzymol 350:87–96. https://doi.org/10.1016/S0076-6879(02)50957-5

Gold ND, Gowen CM, Lussier FX, Cautha SC, Mahadevan R, Martin VJJ (2015) Metabolic engineering of a tyrosine-overproducing yeast platform using targeted metabolomics. Microb Cell Fact 14:73. https://doi.org/10.1186/s12934-015-0252-2

Graham LD, Gillies FM, Coggins JR (1993) Over-expression of the yeast multifunctional arom protein. Biochim Biophys Acta 1216(3):417–424

Hartmann M, Schneider TR, Pfeil A, Heinrich G, Lipscomb WN, Braus GH (2003) Evolution of feedback-inhibited beta/alpha barrel isoenzymes by gene duplication and a single mutation. Proc Natl Acad Sci USA 100(3):862–867. https://doi.org/10.1073/pnas.0337566100

Hegemann JH, Heick SB (2011) Delete and repeat: a comprehensive toolkit for sequential gene knockout in the budding yeast *Saccharomyces cerevisiae*. Methods Mol Biol 765:189–206. https://doi.org/10.1007/978-1-61779-197-0_12

Iraqui I, Vissers S, Cartiaux M, Urrestarazu A (1998) Characterisation of *Saccharomyces cerevisiae ARO8* and *ARO9* genes encoding aromatic aminotransferases I and II reveals a new aminotransferase subfamily. Mol Gen Genet 257(2):238–248

Jiang H, Morgan JA (2004) Optimization of an in vivo plant P450 monooxygenase system in *Saccharomyces cerevisiae*. Biotechnol Bioeng 85(2):130–137. https://doi.org/10.1002/bit.10867

Karsten WE, Reyes ZL, Bobyk KD, Cook PF, Chooback L (2011) Mechanism of the aromatic aminotransferase encoded by the *Aro8* gene from *Saccharomyces cerevisiae*. Arch Biochem Biophys 516(1):67–74. https://doi.org/10.1016/j.abb.2011.09.008

Koopman F, Beekwilder J, Crimi B, van Houwelingen A, Hall RD, Bosch D, van Maris AJA, Pronk JT, Daran JM (2012) De novo production of the flavonoid naringenin in engineered *Saccharomyces cerevisiae*. Microb Cell Fact 11:155. https://doi.org/10.1186/1475-2859-11-155

Krivoruchko A, Nielsen J (2015) Production of natural products through metabolic engineering of *Saccharomyces cerevisiae*. Curr Opin Biotechnol 35:7–15. https://doi.org/10.1016/j.copbio.2014.12.004

Kyndt JA, Meyer TE, Cusanovich MA, Van Beeumen JJ (2002) Characterization of a bacterial tyrosine ammonia lyase, a biosynthetic enzyme for the photoactive yellow protein. FEBS Lett 512(1–3):240–244. https://doi.org/10.1016/S0014-5793(02)02272-X

Li MJ, Kildegaard KR, Chen Y, Rodriguez A, Borodina I, Nielsen J (2015) *De novo* production of resveratrol from glucose or ethanol by engineered *Saccharomyces cerevisiae*. Metab Eng 32:1–11. https://doi.org/10.1016/j.ymben.2015.08.007

Liu D, Li BZ, Liu H, Guo XJ, Yuan YJ (2017) Profiling influences of gene overexpression on heterologous resveratrol production in *Saccharomyces cerevisiae*. Front Chem Sci Eng 11(1):117–125. https://doi.org/10.1016/j.meteno.2015.09.001

Liu QL, Liu HJ, Yang YY, Zhang XM, Bai YL, Qiao MQ, Xu HJ (2014) Scarless gene deletion using *mazF* as a new counter-selection marker and an improved deletion cassette assembly method in *Saccharomyces cerevisiae*. J Gen Appl Microbiol 60(2):89–93. https://doi.org/10.2323/jgam.60.89

Luttik MA, Vuralhan Z, Suir E, Braus GH, Pronk JT, Daran JM (2008) Alleviation of feedback inhibition in *Saccharomyces cerevisiae* aromatic amino acid biosynthesis: quantification of metabolic impact. Metab Eng 10(3–4):141–153. https://doi.org/10.1016/j.ymben.2008.02.002

Mao JW, Liu QL, Song XF, Wang HSY, Feng H, Xu HJ, Qiao MQ (2017) Combinatorial analysis of enzymatic bottlenecks of L-tyrosine pathway by *p*-coumaric acid production in *Saccharomyces cerevisiae*. Biotechnol Lett 39(7):977–982. https://doi.org/10.1007/s10529-017-2322-5

Ohashi K, Chaleckis R, Takaine M, Wheelock CE, Yoshida S (2017) Kynurenine aminotransferase activity of *Aro8/Aro9* engage tryptophan degradation by producing kynurenic acid in *Saccharomyces cerevisiae*. Sci Rep 7(1):12180. https://doi.org/10.1038/s41598-017-12392-6

Paravicini G, Mosch HU, Schmidheini T, Braus G (1989) The general control activator protein GCN4 is essential for a basal level of *ARO3* gene expression in *Saccharomyces cerevisiae*. Mol Cell Biol 9(1):144–151

Rodriguez A, Kildegaard KR, Li MJ, Borodina I, Nielsen J (2015) Establishment of a yeast platform strain for production of *p*-coumaric acid through metabolic engineering of aromatic amino acid biosynthesis. Metab Eng 31:181–188. https://doi.org/10.1016/j.ymben.2015.08.003

Romagnoli G, Knijnenburg TA, Liti G, Louis EJ, Pronk JT, Daran JM (2015) Deletion of the *Saccharomyces cerevisiae ARO8* gene, encoding an aromatic amino acid transaminase, enhances phenylethanol production from glucose. Yeast 32(1):29–45. https://doi.org/10.1002/yea.3015

Sato F, Inui T, Takemura T (2007) Metabolic engineering in isoquinoline alkaloid biosynthesis. Curr Pharm Biotechnol 8(4):211–218. https://doi.org/10.2174/138920107781387438

Sauer B (1987) Functional expression of the cre-lox site-specific recombination system in the yeast *Saccharomyces cerevisiae*. Mol Cell Biol 7(6):2087–2096

Silva S, Costa EM, Calhau C, Morais RM, Pintado ME (2017) Anthocyanin extraction from plant tissues: a review. Crit Rev Food Sci Nutr 57(14):3072–3083. https://doi.org/10.1080/10408398.2015.1087963

Strucko T, Magdenoska O, Mortensen UH (2015) Benchmarking two commonly used *Saccharomyces cerevisiae* strains for heterologous vanillin-β-glucoside production. Metab Eng Commun 2:99–108. https://doi.org/10.1016/j.meteno.2015.09.001

Vuralhan Z, Luttik MA, Tai SL, Boer VM, Morais MA, Schipper D, Almering MJ, Kotter P, Dickinson JR, Daran JM, Pronk JT (2005)

Physiological characterization of the *ARO10*-dependent, broad-substrate-specificity 2-oxo acid decarboxylase activity of *Saccharomyces cerevisiae*. Appl Environ Microbiol 71(6):3276–3284. https://doi.org/10.1128/AEM.71.6.3276-3284.2005

Xu P, Bhan N, Koffas MAG (2013) Engineering plant metabolism into microbes: from systems biology to synthetic biology. Curr Opin Biotech 24(2):291–299. https://doi.org/10.1016/j.copbio.2012.08.010

Yao LH, Jiang YM, Shi J, Tomas-Barberan FA, Datta N, Singanusong R, Chen SS (2004) Flavonoids in food and their health benefits. Plant Food Hum Nutr 59(3):113–122. https://doi.org/10.1007/s11130-004-0049-7